

Kinetic and Mechanistic Studies of the Reactions of Diarylgermylenes and Tetraaryldigermenes with Carbon Tetrachloride

L. A. Huck and W. J. Leigh*

- Figure S1.** 600 MHz ^1H NMR spectrum of a 0.02 M solution of **6a** in C_6D_{12} containing CCl_4 (0.05 M) and Si_2Me_6 (3 mM) before (*top*) and after 254 nm photolysis for 200s (*bottom*). S3
- Figure S2.** Concentration vs. time plots from steady state photolysis of **6a** (0.02 M, ●) in deoxygenated C_6D_{12} containing various concentrations of CCl_4 ((a) 0.006 M; (b) 0.02 M; (c) 0.05 M; (d) 0.10 M) as determined by ^1H NMR spectroscopy; **10** (■), **11** (○), **12** (Δ), and DMB (□). S4
- Figure S3.** 600 MHz ^1H NMR spectrum of a 0.02 M solution of **6a** in $\text{THF-}d_8$ containing CCl_4 (0.05 M) and Si_2Me_6 (3 mM) before (*top*) and after photolysis for 200 s with 254 nm light (*bottom*). S5
- Figure S4.** Concentration vs. time plots from steady state photolysis of **6a** (0.021 M, ●) in deoxygenated $\text{THF-}d_8$ containing CCl_4 (0.05 M) as determined by ^1H NMR spectroscopy; **10** (■), **11** (○), **12** (Δ), and DMB (□). S6
- Figure S5.** Select regions of the ^1H NMR spectrum (C_6D_6) of the products of CCl_4 quenching of **9g**. $\text{Mes}_4\text{Ge}_2\text{Cl}_2$ is only present in roughly 20% yield. S6
- Figure S6.** Plots of k_{decay} vs. $[\text{CCl}_4]$ for (a) **8a** and (b) **9a** in deoxygenated hexanes and (c) the **8a**-THF complex in THF at 25 °C. S7
- Figure S7.** Plots of k_{decay} vs. $[\text{CCl}_4]$ for (a) **8b** and (b) **9b** in deoxygenated hexanes and (c) the **8b**-THF complex in THF at 25 °C. S7
- Figure S8.** Plots of k_{decay} vs. $[\text{CCl}_4]$ for (a) **8c** and (b) **9c** in deoxygenated hexanes and (c) the **8c**-THF complex in THF at 25 °C. S7
- Figure S9.** Plots of k_{decay} vs. $[\text{CCl}_4]$ for (a) **8d** and (b) **9d** in deoxygenated hexanes and (c) the **8d**-THF complex in THF at 25 °C. S8
- Figure S10.** Plots of k_{decay} vs. $[\text{CCl}_4]$ for (a) **8e** and (b) **9e** in deoxygenated hexanes and (c) the **8e**-THF complex in THF at 25 °C. S8
- Figure S11.** Plots of k_{decay} vs. $[\text{CCl}_4]$ for (a) **8f** and (b) **9f** in deoxygenated hexanes and (c) the **8f**-THF complex in THF at 25 °C. S8
- Figure S12.** Transient absorption spectra recorded by laser flash photolysis of a 3 mM solution of 3,4-dimethyl-1,1-bis[3-fluorophenyl]germacyclopent-3-ene (**6e**) in deoxygenated THF, recorded 0.80-1.28 μs (circle) and 35.7-36.6 μs (square) after the laser pulse. The inset shows transient absorption vs. time profiles recorded at 340 nm S9

(**8e**-THF) and 440 nm (**9e**).

Figure S13. Plot of k_{decay} vs. $[\text{CHCl}_3]$ for the reaction of the **8a**-THF complex with CHCl_3 in THF at 25.0 °C. S9

Figure S14. Plot of k_{decay} vs. $[\text{CCl}_4]$ for the reaction of digermene **9g** with CCl_4 in deoxygenated hexanes at 25.0 °C. S10

Figure S15. Plots of k_{decay} vs. $[\text{Q}]$ for the reaction of (a) **8a** and (b) **9a** with CCl_4 in dry, deoxygenated hexanes at 12 °C (○), 25 °C (□), 32 °C (●), 46 °C (■) and 60 °C (Δ). The rate constants are listed in Table S1. S10

Figure S16. Plots of k_{decay} vs. $[\text{Q}]$ for the reaction of **8a-THF** with CCl_4 in dry, deoxygenated THF at 10 °C (○), 25 °C (Δ), 55 °C (□), and 62 °C (◇). The rate constants are listed in Table S1. S11

Table S1 – Absolute rate constants for the reactions of **8a** and **9a** with carbon tetrachloride in dry, deoxygenated hexanes for the reactions of **8a-THF** with carbon tetrachloride in dry, deoxygenated THF at various temperatures. The rate constants have been corrected to account for the change in density of the solvents with temperature. Errors are reported as $\pm 2\sigma$. S11

Figure S17. ORTEP diagram of **14** (50% probability ellipsoids). H atoms omitted for clarity. S11

Table S2. Crystal data and structure refinement for **14** (CCDC 788625) S12

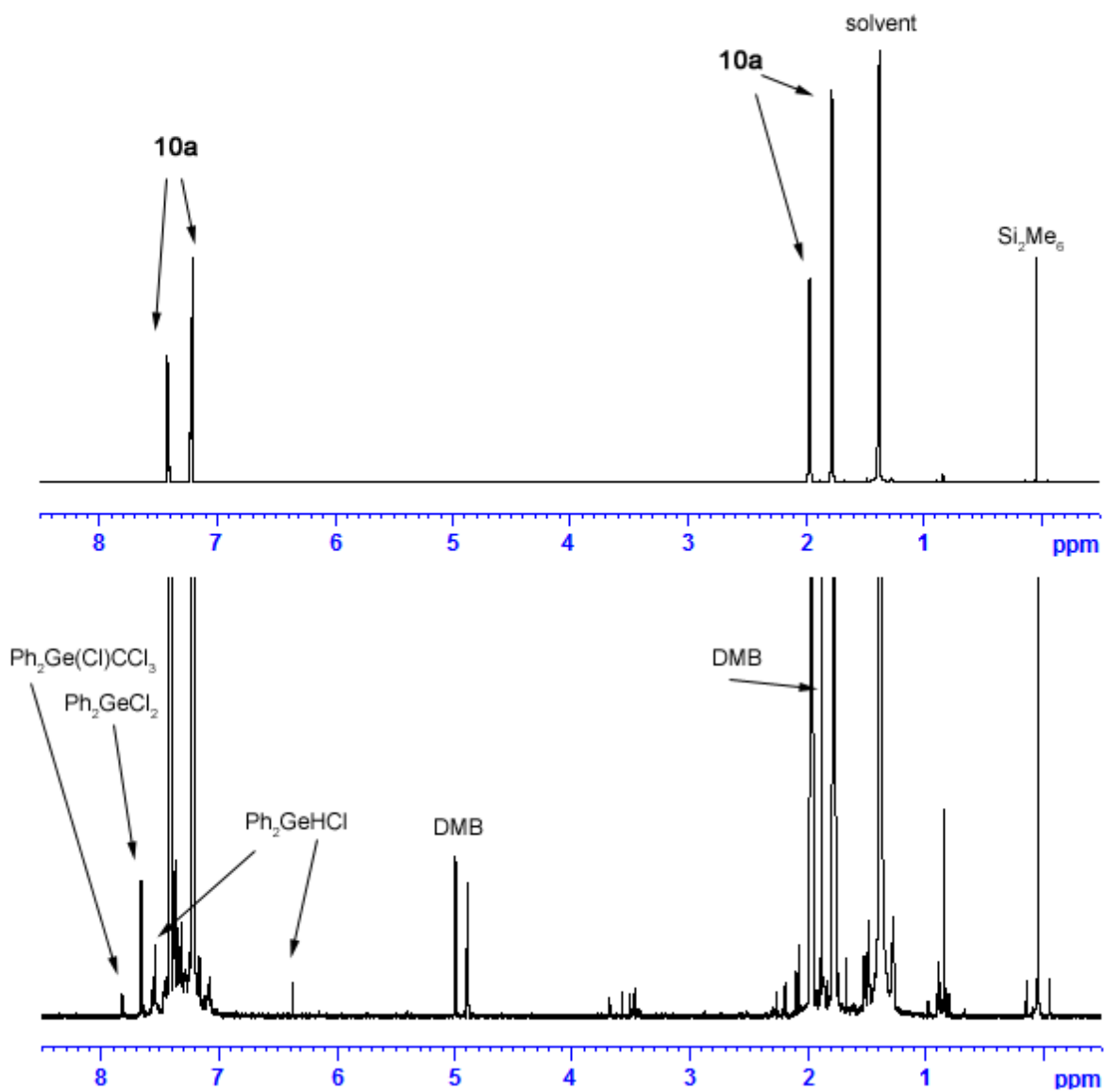


Figure S1. 600 MHz ^1H NMR spectrum of a 0.02 M solution of **6a** in C_6D_{12} containing CCl_4 (0.05 M) and Si_2Me_6 (3 mM) before (*top*) and after 254 nm photolysis for 200s (*bottom*).

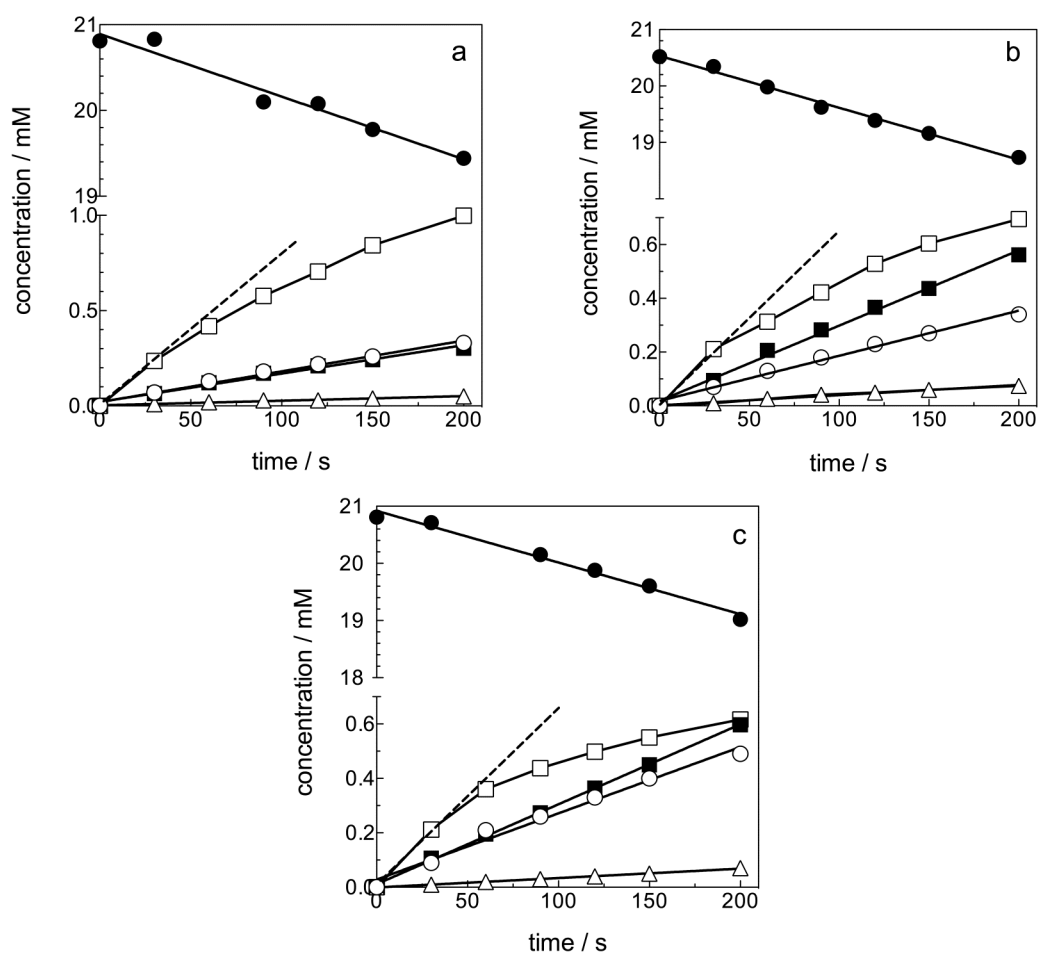


Figure S2. Concentration vs. time plots from steady state photolysis of **6a** (0.02 M, ●) in deoxygenated C₆D₁₂ containing various concentrations of CCl₄ ((a) 0.02 M; (b) 0.05 M; (c) 0.10 M) as determined by ¹H NMR spectroscopy; **10** (■), **11** (○), **12** (△), and DMB (□).

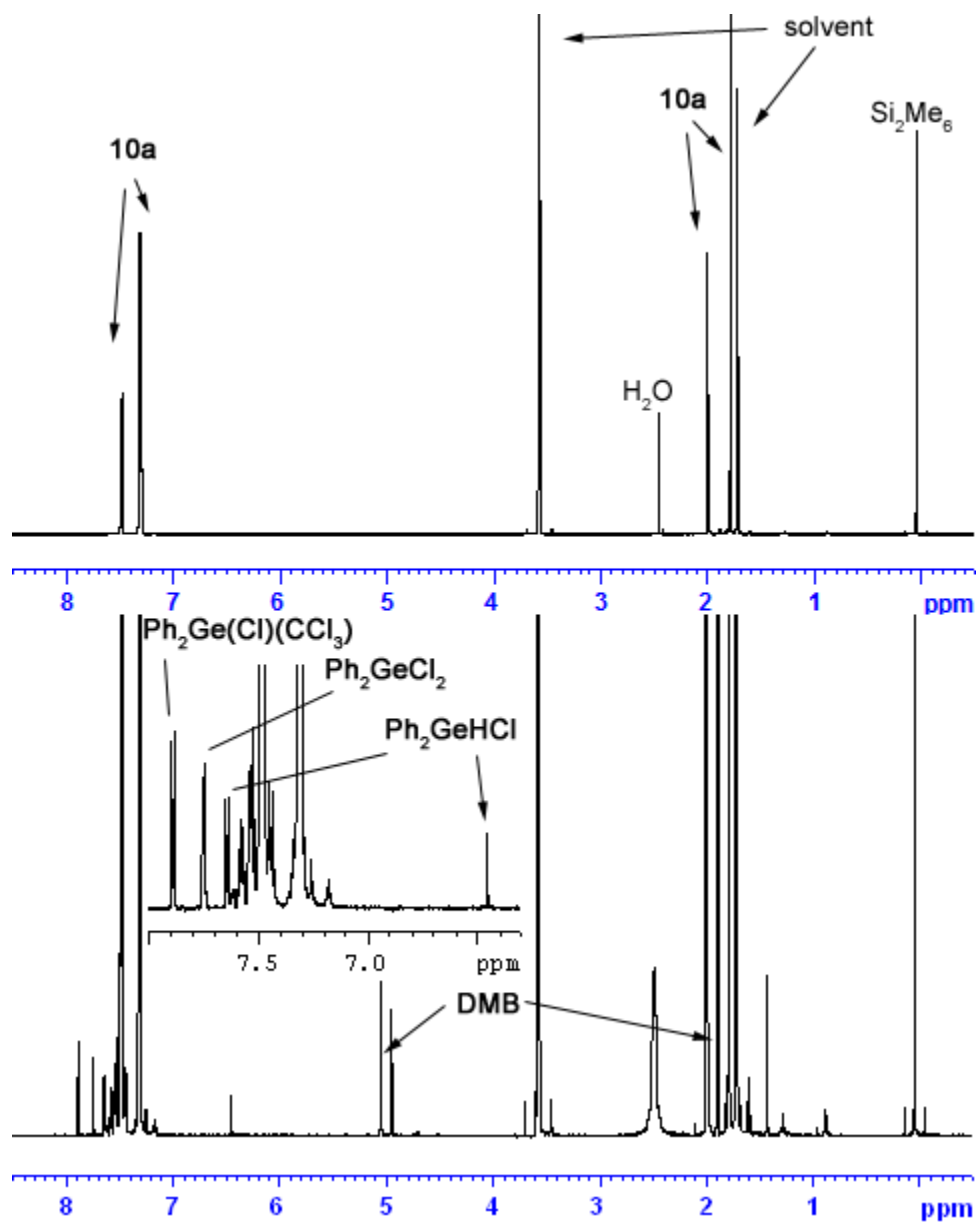


Figure S3. 600 MHz ^1H NMR spectrum of a 0.02 M solution of **6a** in THF- d_8 containing CCl_4 (0.05 M) and Si_2Me_6 (3 mM) before (*top*) and after photolysis for 200 s with 254 nm light (*bottom*).

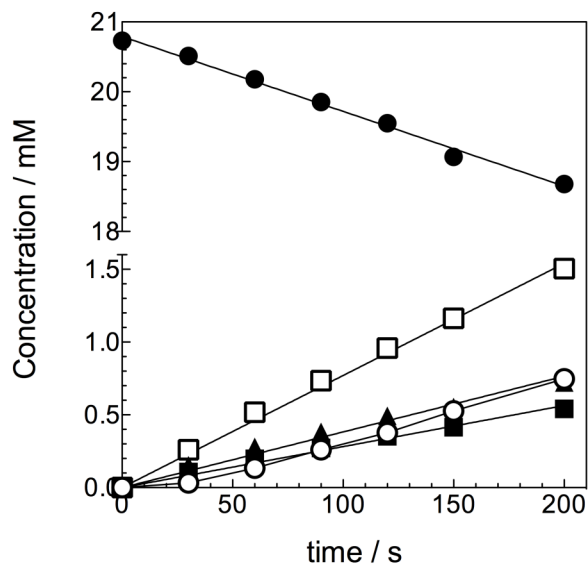


Figure S4. Concentration vs. time plots from steady state photolysis of **6a** (0.021 M, ●) in deoxygenated THF- d_8 containing CCl_4 (0.05 M) as determined by ^1H NMR spectroscopy; **10** (■), **11** (○), **12** (Δ), and DMB (□).

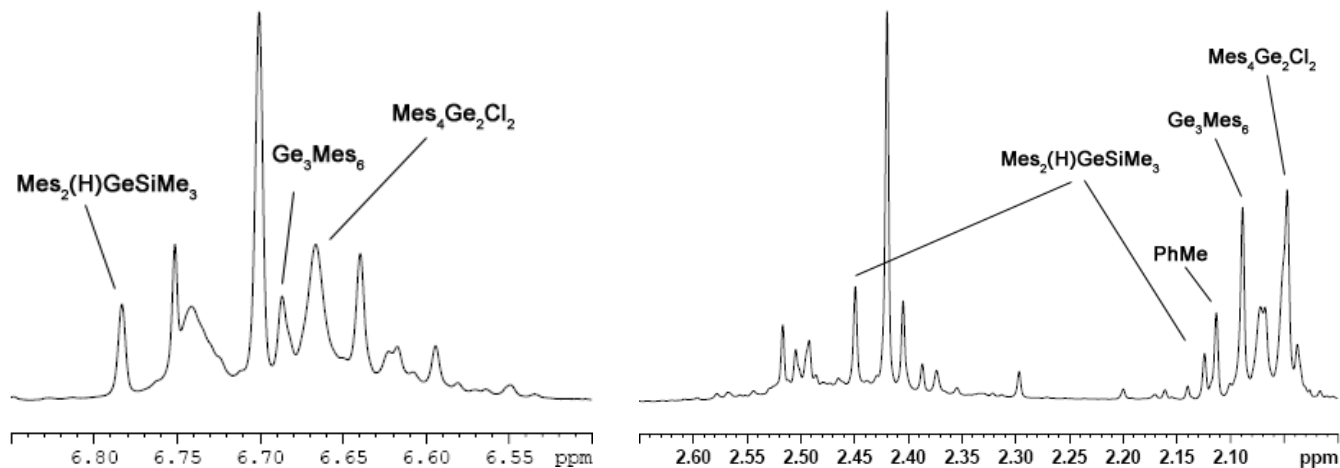


Figure S5. Select regions of the ^1H NMR spectrum (C_6D_6) of the products of CCl_4 quenching of **9g**. $\text{Mes}_4\text{Ge}_2\text{Cl}_2$ is present in roughly 20% yield.

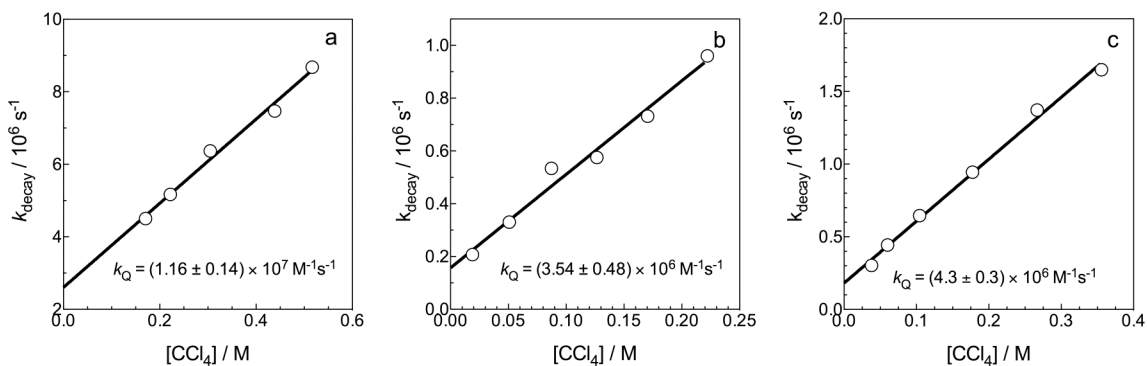


Figure S6. Plots of k_{decay} vs. $[\text{CCl}_4]$ for (a) **8a** and (b) **9a** in deoxygenated hexanes and (c) the **8a**-THF complex in THF at 25 °C.

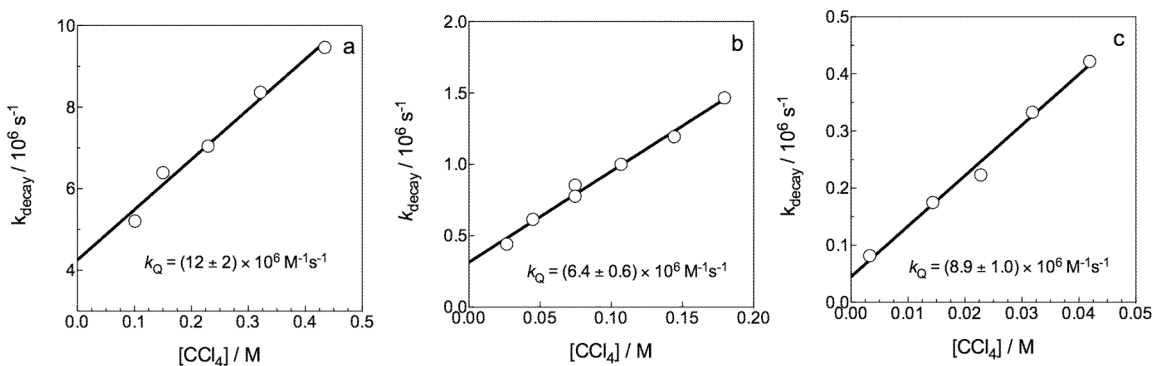


Figure S7. Plots of k_{decay} vs. $[\text{CCl}_4]$ for (a) **8b** and (b) **9b** in deoxygenated hexanes and (c) the **8b**-THF complex in THF at 25 °C.

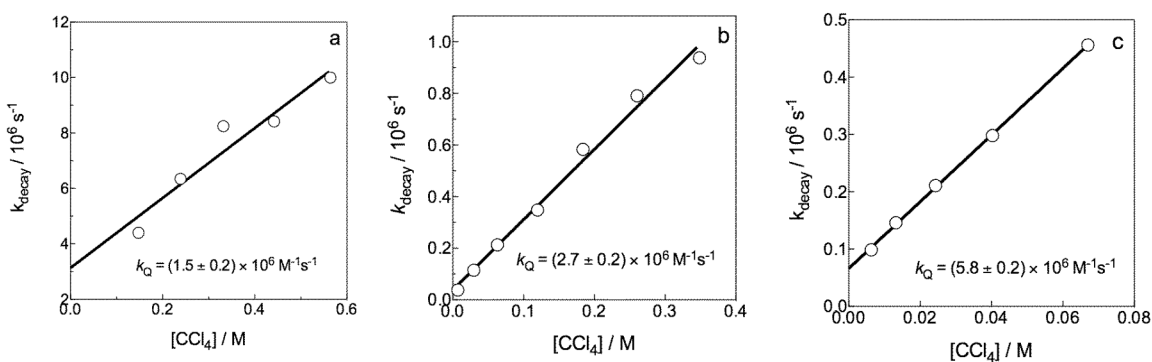


Figure S8. Plots of k_{decay} vs. $[\text{CCl}_4]$ for (a) **8c** and (b) **9c** in deoxygenated hexanes and (c) the

8c-THF complex in THF at 25 °C.

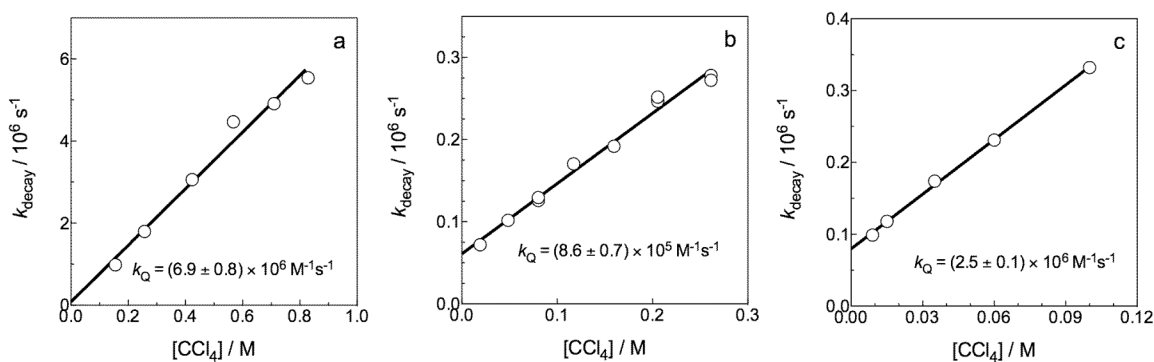


Figure S9. Plots of k_{decay} vs. $[\text{CCl}_4]$ for (a) **8d** and (b) **9d** in deoxygenated hexanes and (c) the **8d**-THF complex in THF at 25 °C.

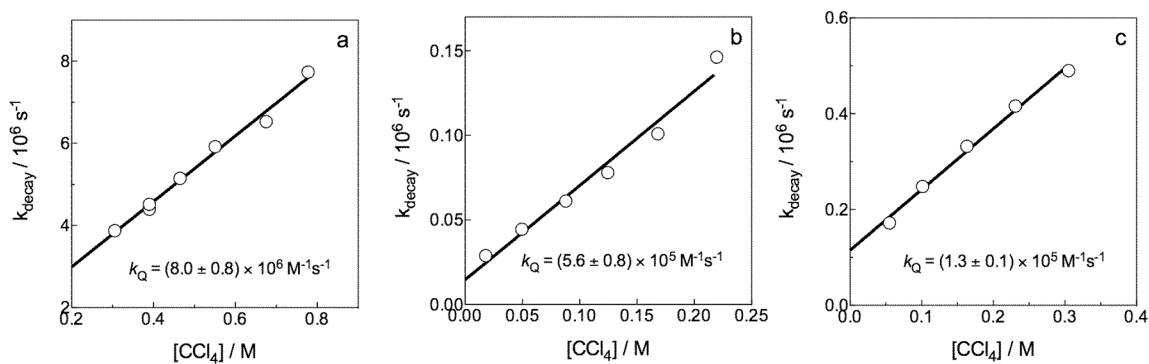


Figure S10. Plots of k_{decay} vs. $[\text{CCl}_4]$ for (a) **8e** and (b) **9e** in deoxygenated hexanes and (c) the **8e**-THF complex in THF at 25 °C.

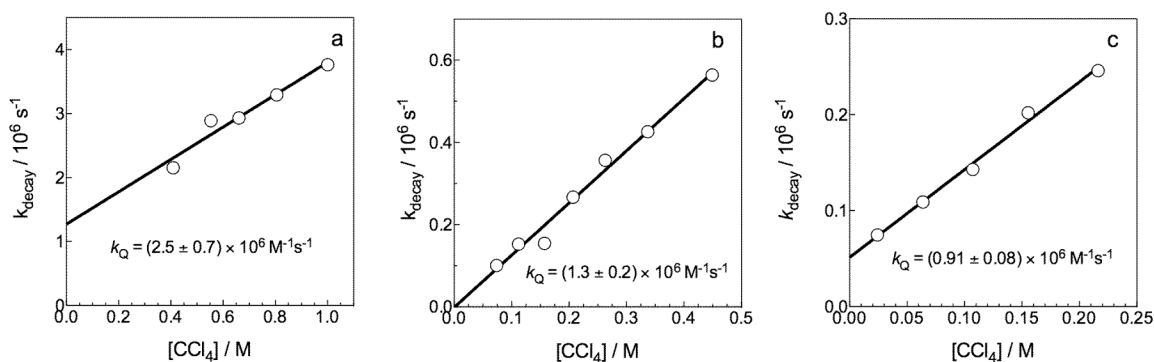


Figure S11. Plots of k_{decay} vs. $[\text{CCl}_4]$ for (a) **8f** and (b) **9f** in deoxygenated hexanes and (c) the **8f**-THF complex in THF at 25 °C.

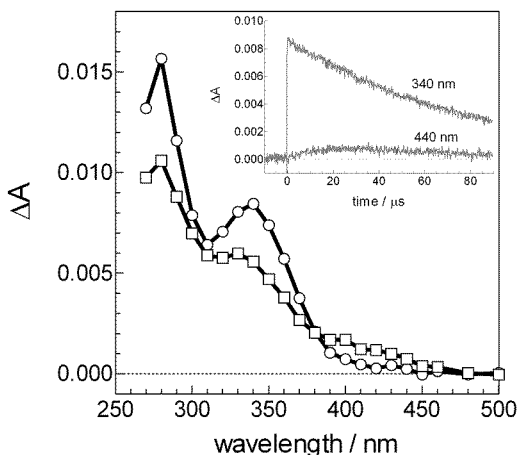


Figure S12. Transient absorption spectra recorded by laser flash photolysis of a 3 mM solution of 3,4-dimethyl-1,1-bis[3-fluorophenyl]germacyclopent-3-ene (**6e**) in deoxygenated THF, recorded 0.80-1.28 μs (circle) and 35.7-36.6 μs (square) after the laser pulse. The inset shows transient absorption vs. time profiles recorded at 340 nm (**8e**-THF) and 440 nm (**9e**).

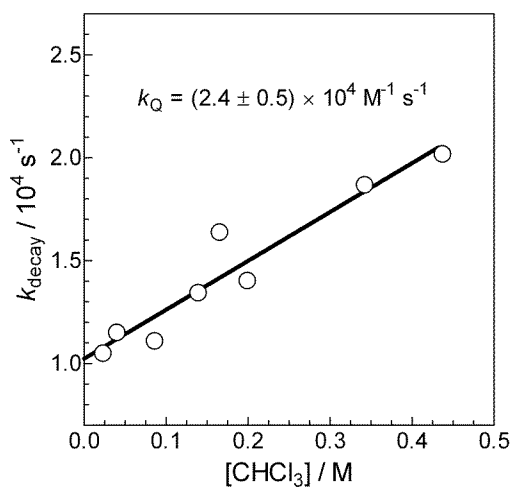


Figure S13. Plot of k_{decay} vs. $[\text{CHCl}_3]$ for the reaction of the **8a**-THF complex with CHCl_3 in THF at 25.0 °C.

Figure S14. Plot of k_{decay} vs. $[\text{CCl}_4]$ for the reaction of digermene **9g** with CCl_4 in deoxygenated hexanes at 25.0 °C.

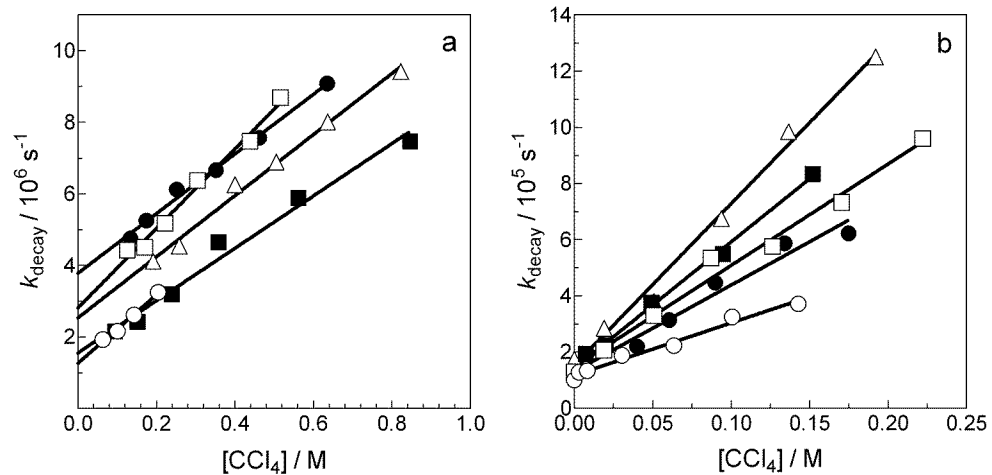
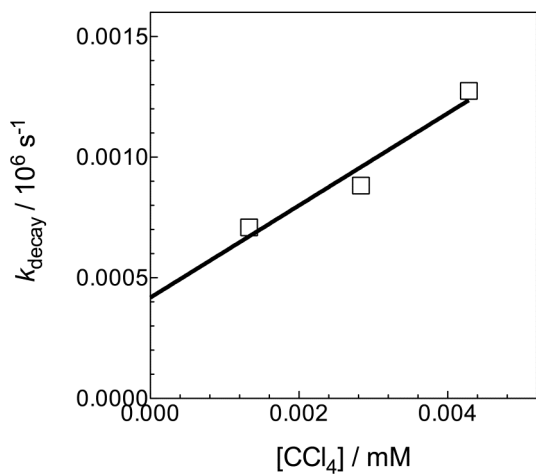


Figure S15. Plots of k_{decay} vs. $[\text{Q}]$ for the reaction of (a) **8a** and (b) **9a** with CCl_4 in dry, deoxygenated hexanes at 12 °C (O), 25 °C (□), 32 °C (•), 46°C (■) and 60 °C (Δ). The rate constants are listed in Table S1.

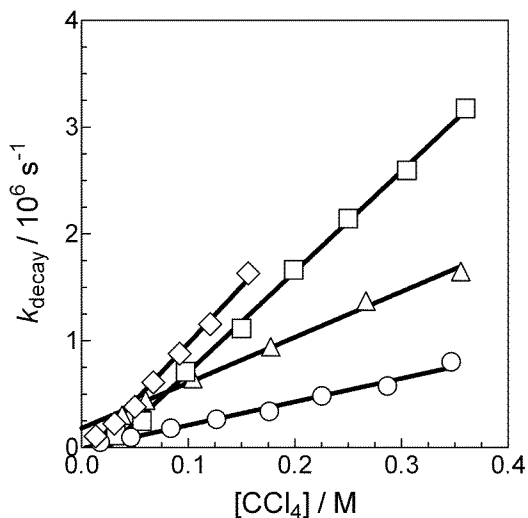


Figure S16. Plots of k_{decay} vs. $[Q]$ for the reaction of **8a-THF** with CCl_4 in dry, deoxygenated THF at 10 °C (O), 25 °C (Δ), 55 °C (\square), and 62 °C (\diamond). The rate constants are listed in Table S1.

Table S1 – Absolute rate constants for the reactions of **8a** and **9a** with carbon tetrachloride in dry, deoxygenated hexanes for the reactions of **8a-THF** with carbon tetrachloride in dry, deoxygenated THF at various temperatures. The rate constants have been corrected to account for the change in density of the solvents with temperature. Errors are reported as $\pm 2\sigma$.

T / °C	$k_{\text{CCl}_4 \text{8a}} / 10^6 \text{ M}^{-1} \text{ s}^{-1}$	$k_{\text{CCl}_4 \text{9a}} / 10^6 \text{ M}^{-1} \text{ s}^{-1}$	T / °C	$k_{\text{CCl}_4 \text{8a-THF}} / 10^6 \text{ M}^{-1} \text{ s}^{-1}$
12.2	9.4 ± 1.2	1.8 ± 0.3	10.3	2.2 ± 0.4
25.0	10.8 ± 1.2	3.5 ± 0.7	25.0	4.3 ± 0.6
32.0	8.4 ± 0.8	3.1 ± 0.7	57.7	9.8 ± 0.6
47.5	7.4 ± 1.0	4.7 ± 0.3	62.4	12 ± 1.2
60.0	9.0 ± 0.7	6.1 ± 0.5		

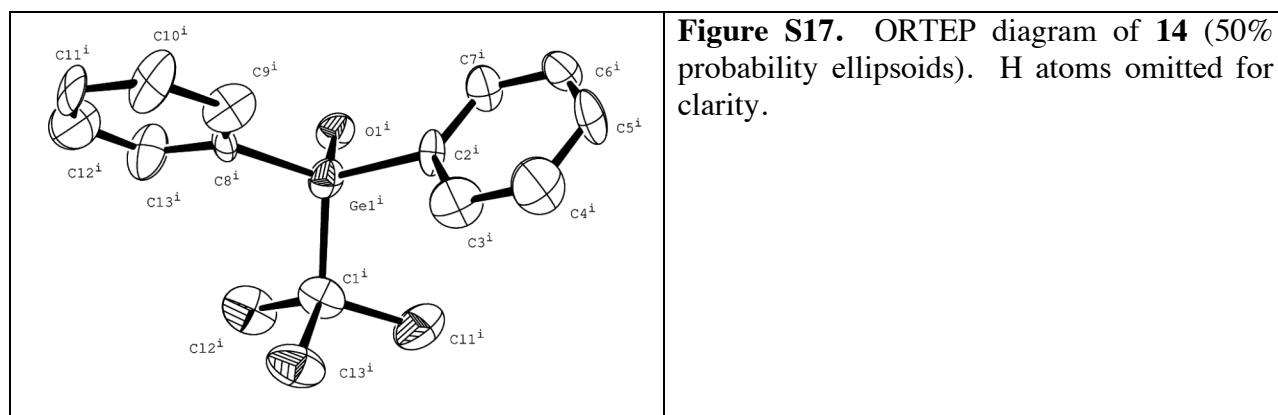


Table S2. Crystal data and structure refinement for **14** (CCDC 788625)

Identification code	CCDC 788625
Empirical formula	C ₁₃ H ₁₁ Cl ₃ GeO
Temperature	173(2) K
Wavelength	0.71073 Å
Formula weight	362.16
Crystal system	Triclinic
Space group	P-1
Unit cell dimensions	$a = 13.651(5)$ Å, $\alpha = 88.545(8)^\circ$ $b = 14.244(5)$ Å, $\beta = 85.854(8)^\circ$ $c = 15.712(5)$ Å, $\gamma = 84.987(7)^\circ$
Volume	3035.0(19) Å ³
Z	8
Density (calculated)	1.585 Mg/m ³
Absorption coefficient	2.531 mm ⁻¹
F(000)	1440
Crystal size	0.40 × 0.30 × 0.10 mm ³
Theta range for data collection	1.30 to 20.87°
Index ranges	-12 ≤ h ≤ 13, -14 ≤ k ≤ 14, -11 ≤ l ≤ 15
Reflections collected	21095
Independent reflections	6337 [R(int) = 0.2301]
Completeness to theta = 20.87°	99.0 %
Absorption correction	Numerical
Max. and min. transmission	0.7859 and 0.4308
Refinement method	Full-matrix least-squares on F ²
Data / restraints / parameters	6337 / 15 / 601
Goodness-of-fit on F ²	0.956
Final R indices [I > 2σ(I)]	R1 = 0.0681, wR2 = 0.1129
R indices (all data)	R1 = 0.2014, wR2 = 0.1536
Largest diff. peak and hole	0.589 and -0.697 e.Å ⁻³